A high frame rate, 340 GHz 3D imaging radar for security

Duncan A. Robertson[1], David G. Macfarlane[1], Robert I. Hunter[1], Scott L. Cassidy[1], Nuria Llombart[2], Erio Gandini[2], Tomas Bryllert[3], Mattias Ferndahl[4], Hannu Lindström[5], Jussi Tenhunen[5], Hannu Vasama[5], Jouni Huopana[6], Timo Selkälä[6], Antti-Jussi Vuotikka[6]

[1] School of Physics & Astronomy, University of St Andrews, St Andrews, Scotland
[2] Technical University of Delft, Delft, Netherlands
[3] Wasa Millimeter Wave AB, Gothenburg, Sweden
[4] GotMIC AB, Gothenburg, Sweden
[5] VTT Technical Research Centre of Finland Ltd., Oulu, Finland
[6] Global Boiler Works Oy, Oulu, Finland
Email: dar@st-and.ac.uk

***Abstract*—The need for improved security at airports with high detection performance, high throughput rates and an improved passenger experience is motivating research into new sensing technologies. The European Union funded CONSORTIS project is addressing these aims by demonstrating a system which combines a submillimeter wave radar, a dual-band passive submillimeter wave camera and automatic anomaly detection software for reliable detection while ensuring passenger privacy. In this paper we describe the 340 GHz 16-channel FMCW radar which produces 3D maps of the subject with ~1 cm^3 voxel resolution over a 1 m^3 sense volume at multi-hertz frame rates. The radar combines advanced transceiver electronics with high speed mechanical beam steering and parallelized processing to achieve this level of performance.**

I. INTRODUCTION

Millimeter wave body scanning portals are now a familiar presence in airports and transport hubs worldwide, complementing archway metal detectors and x-ray baggage scanners [1]. The most widely deployed millimeter wave body scanners are the L-3 ProVision [2] (~26 GHz cylindrical scan synthetic aperture radar), the Smith Eqo [3] (24 GHz CW radar with reconfigurable reflectarry antennas), and the Rohde & Schwarz QPS [4] (77 GHz FMCW radar with MIMO array antennas). Despite the wide deployment of these systems, airports desire improved security technology that could provide higher throughput rates, higher detection performance and an enhanced passenger experience. In 2011, the European Union solicited proposals to reduce the time needed for security checks while maintaining or increasing the level of detection under FP7 Topic SEC-2012.3.4.5-5 “Further research and pilot implementation of Terahertz detection techniques (T-Ray)”. Project proposals were expected to develop a prototype imaging system operating at a single or multiple sub/millimeter wave frequencies, including frequencies above 300 GHz, which had to be safe for use on the general public and allow concepts of operation which respect privacy.

The CONSORTIS (Concealed Object Stand-Off Real-Time Imaging for Security) project [5], funded under the above EU scheme, aims to demonstrate high resolution, real time security imaging with significantly improved throughput rates. The full CONSORTIS system combines a 340 GHz 3D imaging radar, a dual-band passive submillimeter wave camera, and automatic anomaly detection (AAD) software to ensure privacy. Only the radar subsystem is discussed in this paper. Submillimeter wave radar can image subjects in 3D with high volumetric resolution combined with penetration through fabrics such that even quite small objects, including non-metallic items, can be resolved under clothing [6, 7, 8, 9].

The CONSORTIS radar is designed to achieve a high volumetric resolution (~1 cm^3) over a substantial target volume (1 x 1 x 1 m^3) at a relatively short working distance, with high frame rate and high dynamic range [10]. The objective is to recover high resolution 3D maps of people as they pass by the system which can be analyzed to identify anomalous objects. The radar has 16 homodyne FMCW channels with frequency multiplying transceivers which exploit self-mixing multiplier technology removing the need for explicit duplexing components, thus greatly simplifying the design.

The radar must cope with dynamic scenes so a high frame rate is essential. Imaging a cubic meter volume with ~cm^3 voxel resolution using 16 radar channels at many frames per second clearly requires high speed beam steering. As non-mechanical beam steering methods such as phased arrays or reconfigurable reflectarrays are still not practical at 340 GHz we have opted to use mechanical beam steering. The sparse focal plane array of transceivers images the target volume via Dragonian focusing mirror optics and a combination of a high speed, double-disc Lissajous scanner in azimuth and a reciprocating mirror in elevation. The opto-mechanical beam scanning is capable of scanning the 1 x 1 m^2 field of view at a 10 Hz refresh rate. Fig. 1 shows a block diagram of the radar.

In this paper the principal hardware modules are presented in section II, the signal and data processing aspects are described in section III, and some example imagery is shown in section IV.

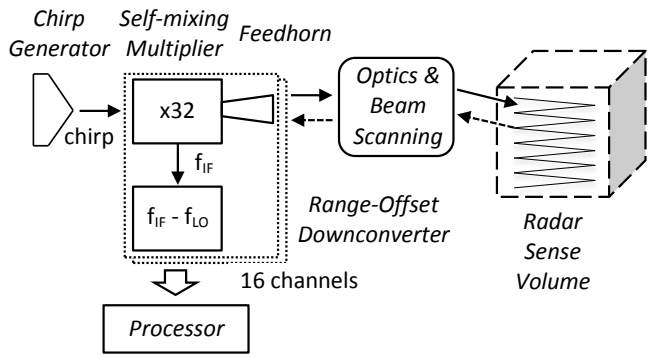

Fig. 1. Block diagram of CONSORTIS 16 channel 340 GHz radar.

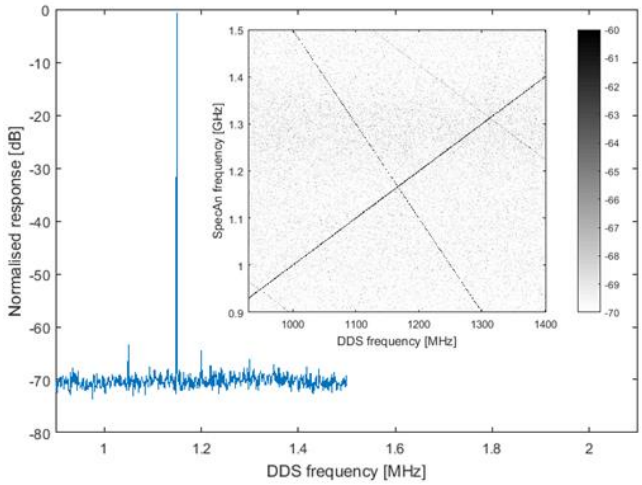

Fig. 2. DDS CW output spectrum with -50 dBc spur free dynamic range (main) and spectrogram of output spectrum versus CW frequency from 930 – 1400 MHz (inset).

II. Radar Hardware

A. FMCW Chirp Generation

The output center frequency of the radar is 340 GHz with a chirp bandwidth of 30 GHz to achieve 0.5 cm range bins. The frequency multiplication factor is x32 so chirps are generated at 10.625 GHz with a bandwidth of 937.5 MHz, i.e. ~9% fractional bandwidth. To achieve fast chirps (40.96 µs) with high linearity and low phase noise, we use a customized Analog Devices AD9914 direct digital synthesis (DDS) evaluation board clocked at 3.5 GHz. The DDS chirp output is upconverted onto a microwave stable local oscillator (STALO) then filtered, frequency doubled, filtered again, amplified and split 16 ways.

The DDS spectral output was characterized over the range 930 – 1400 MHz by recording the output on a spectrum analyzer as a function of DDS CW frequency. This revealed the behavior of the desired output term plus the dominant unwanted spurs, which are typical of DDS signal generation. The resulting spectrogram and one example spectrum are shown in Fig. 2. It can be seen that the three dominant spurs tune in the opposite sense to the main output and the spur free dynamic range (SFDR) is better than -50 dBc which is consistent with the AD9914 specification.

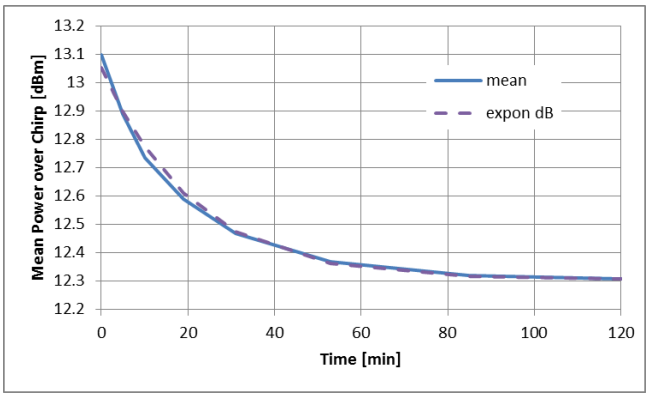

Fig. 3. Chirp generator output mean power over chirp bandwidth versus time during warm up and fitted exponential with 20 minute time constant.

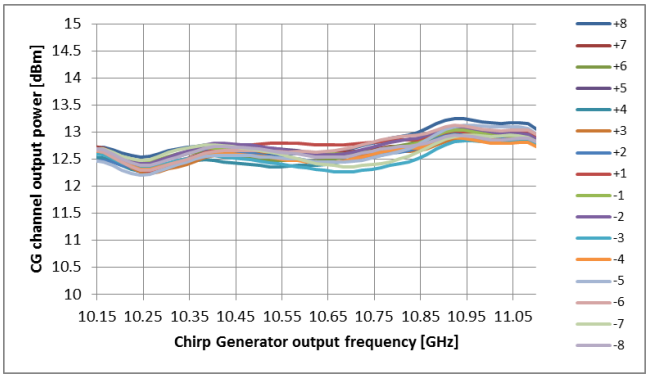

Fig. 4. Chirp generator output power versus frequency for all 16 channels.

The amplitude flatness of the chirp generator is an important quantity since the signal drives the frequency multipliers which are highly nonlinear and have a strict minimum input power requirement of +10.5 dBm to ensure stable operation. The power:frequency response of one output channel of the chirp generator was measured eight times over two hours after switch on to investigate the warmup characteristics. A power meter was used since spectrum analyzers have insufficient amplitude flatness for this type of measurement. Fig. 3 shows the mean power output across the frequency band 10.14 – 11.08 GHz as a function of time. The mean power is fitted well by an exponential decay curve with a time constant of 20 minutes. Overall the variation in output power during warmup is less than 1 dB and the chirp generator reaches within 0.1 dB of its stable value in less than one hour. The power:frequency response was also measured for all 16 channels once warm and the results are shown in Fig. 4. The amplitude flatness is less than ±0.5 dB for all channels and the power output is well above the required minimum value for driving the multipliers.

B. Self-mixing multiplier transceivers

The x32 transceivers use a novel self-mixing multiplier technology in the final stage [11]. The final diode pair acts as both a doubler on transmit and a subharmonic mixer on receive, with the IF coupled out on the Schottky diode bias line. Whilst this slightly compromises the power output and conversion loss compared to a dedicated doubler and mixer

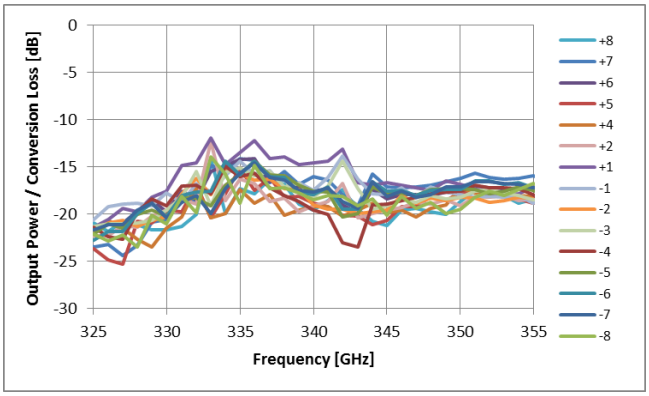

Fig. 5. Transceiver figure of merit, FOM = output power/conversion loss versus output frequency, per channel.

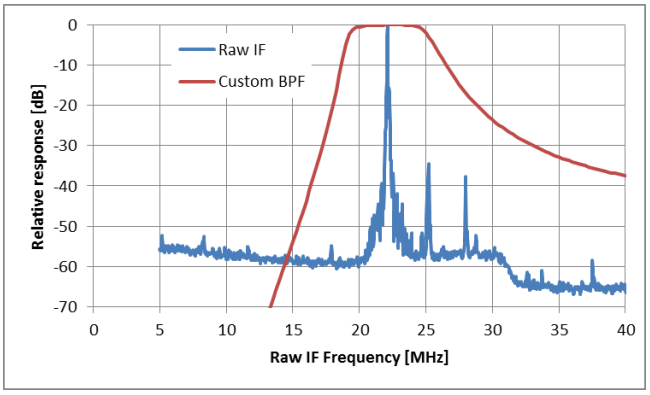

Fig. 6. Raw IF spectrum of point target at focal distance with custom bandpass filter response overlaid.

respectively, the design avoids the need for an external transmit-receive duplexer which is a significant advantage when assembling multi-channel arrays.

The performance of a given transceiver can be expressed by defining a figure of merit, FOM, equal to the ratio of output power (typ. 0 dBm) to conversion loss (typ. -18 dB). This quantity maps directly into the radar equation for each transceiver so can be used to assess channel balance across the array. Values of FOM were calculated from measured values of output power and conversion loss versus frequency for all 16 channels and the results are shown in Fig. 5. The variation in FOM across the chirp bandwidth was $\leq \pm 5$ dB for all channels. In the process of FMCW deramping, the FOM variations across the chirp bandwidth are effectively averaged out so the mean value of FOM can be used to indicate the overall effect on the received IF signal. Taking the mean value of FOM for each transceiver shows all channels fall within the range -19.5 to -16.4 dB. Such a small 3.1 dB variation shows there is excellent channel balance across the array in terms of radar signal throughput.

C. Range-offset Downconversion Receiver

The total distance from each transceiver to the subject focal plane amounts to some 4.46 m of which 2.03 m is the path inside the radar from the transceiver through the optics to the final mirror and 2.43 m is the stand-off distance from the final mirror to the subject focal plane. The raw IF frequency for a 30 GHz 40.96 µs FMCW chirp is thus 21.79 MHz at the focal plane. With a desired range swath of one meter, the front and back edges of the sense volume then correspond to raw IF frequencies of 19.34 and 24.23 MHz respectively. Since there is no need to recover data from ranges closer or further than the sense volume we have employed a range-offset downconversion receiver to bandpass filter the raw IF spectrum and translate it to baseband for subsequent sampling.

The receiver uses an 18 MHz crystal local oscillator with 16 outputs feeding 16 channels of heterodyne downconversion. The desired 1 m range swath is selected from the raw IF spectrum using a custom bandpass filter with a -1 dB passband covering 19.5 to 24.75 MHz. Fig. 6 shows an example raw IF spectrum for a target close the focal distance with the custom bandpass filter response overlaid. The receiver circuit also provides baseband (1 – 6 MHz) amplification and anti-alias low-pass filtering prior to sampling.

D. Focusing and beam steering optics

The transceivers are coupled to free space using smooth-walled E-plane split block feedhorns, which are directly machined in aluminum [10]. The ~25 dBi horns couple to a free-space Gaussian mode with >99% efficiency and maintain a -10 dB beamwidth of 9.75° ± 6.7% over the full 30 GHz bandwidth. The sidelobe level is below -30 dB and agreement between measured far-field patterns and mode matching design simulations is excellent down to below -40 dB. However, it is the mainlobe which is most relevant as the optics are designed using an edge taper of approximately -10 dB.

A pair of elliptical offset reflectors in a Dragonian configuration (primary 385 x 290 mm, secondary 382 x 258 mm) is used to focus the sparse linear array of transceivers onto the subject focal plane with a nominal spot diameter of 1 cm. The Dragonian design was chosen as it offers the best performance with low aberrations and reduced spillover loss for a large focal plane array (~200 mm) and a relatively wide field-of-view (~1 m x 1 m at 3.5 m focal distance, i.e. ~16° x 16°). The optical aperture is modest (~250 mm) so the beam scanning optics can follow the focusing optics.

A rotating double-disc Lissajous scanner performs a high speed azimuth scan in the form of a long, thin figure-of-eight pattern as an approximation to a linear scan. Two lightweight and balanced circular plane mirrors, whose normals are tilted with respect to their rotation axes, counter-rotate to achieve this scan pattern. The two mirrors (diameters 280 and 350 mm) are driven from a single motor via belt and pulley coupling. One rotation of the motor shaft causes one complete figure-of-eight scan and hence two lines in the image; left-to-right and right-to-left. For a 10 Hz frame rate the discs rotate at 2700 rpm / 45 Hz. The vertical extent of the figure-of-eight pattern is less than two beamwidths (<2 cm) so provides adequate spatial sampling despite not being perfectly linear.

The elevation direction is scanned by the primary mirror of the Dragonian pair which reciprocates by ±0.22° to scan each transceiver beam vertically by 53 mm in the subject focal plane. The pivot axis lies parallel to but offset from the minor

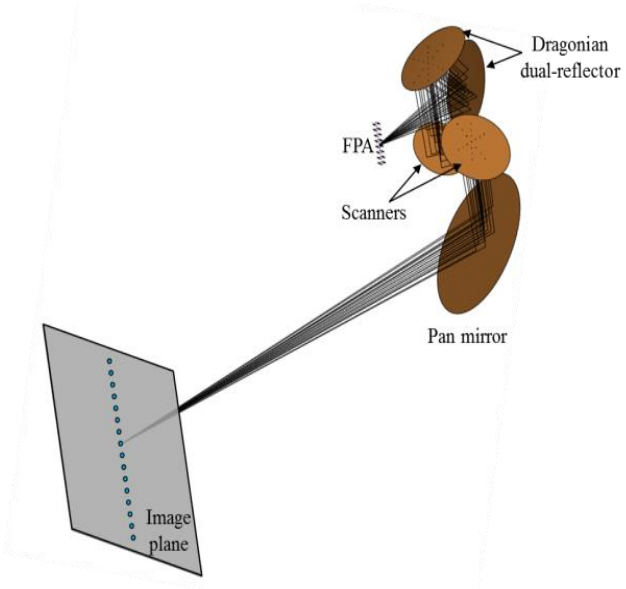

Fig. 7. Ray trace diagram of optical elements with transceiver array and 1 x 1 m2 target focal plane. The 16 yellow dots indicate the nominal positions of each beam imaged from the sparse transceiver array.

axis of the elliptical mirror. The aluminum mirror has ribs and pockets on the rear surface to provide stiffness and minimize weight (1.3 kg) and is balanced about the pivot axis. A pair of linear motors, driven by computer generated analog waveforms, are used in a push-pull configuration to drive the reciprocating motion.

The 1 x 1 m^2 field of view is sampled by 144 x 100 lines of sight (elevation x azimuth). Range profiles measured for each line of sight in a frame are triggered by a shaft encoder on the double-disc scanner motor whose spacing is proportional to the cosine of the shaft angle. This ensures the azimuth points are equally sampled in angle. With 16 transceivers disposed vertica1lly, each transceiver covers 9 lines per frame in elevation, scanned by the reciprocating mirror. The elevation scan drive waveform (nominally a triangle wave) is clocked by a conventional encoder also mounted on the double-disc scanner motor shaft. The motor undergoes 4.5 rotations to complete the 9 line scans of one frame. Due to the combination of the reciprocating elevation scan and the figure-of-eight azimuth scan, up frames and down frames have slightly different non-uniform sampling patterns. The data processing and display takes account of these differences in absolute pointing angles.

The final optical element is the pan mirror, a large elliptical mirror (640 x 460 mm) with a plane surface, which deflects the whole field of view to the left or right to follow subjects as they walk past the system. A ray trace diagram showing all the optical elements, transceiver array and target focal plane is shown in Fig. 7.

III. Signal and Data Processing

The baseband signals are sampled by two 8 channel 16-bit ADC cards running at 25 MSa/s and the data are transferred to the host PC over PCIe. For each line of sight, 1024 samples are

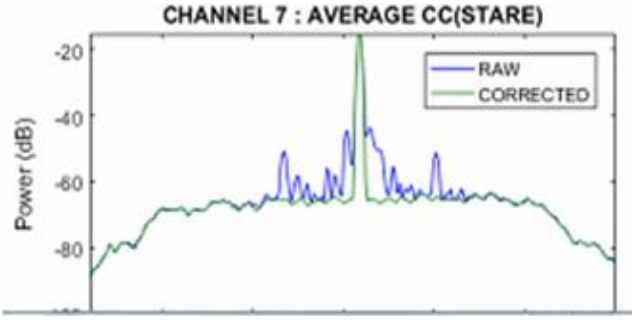

Fig. 8. Raw and corrected range point response for one example channel averaged over 100 chirps.

acquired on each channel and are processed by FFT to yield 512 range bins covering a total range extent of 2.56 m. Whilst this exceeds the distance required for the 1 m deep target volume it allows for the finite roll-off of the swath-defining bandpass filter and anti-alias filter.

The chirp generator and transceivers were designed to minimize amplitude and phase distortion of the transmitted chirp. With such a wide chirp bandwidth some residual nonlinearities remain and the raw range point response of the radar is slightly degraded from the theoretical behavior typically below -20 dBc. Nonetheless, the raw range point response is quite clean for a radar with a 30 GHz chirp bandwidth. To further improve the range point response, we apply amplitude and phase corrections to each channel prior to the FFT, derived from a measurement of a point target at the focal distance. Fig. 8 shows the raw and corrected point response for one example channel, averaged over 100 chirps. The compensation is valid over the 1 m range swath.

To maintain real-time operation, all the data from one frame must be processed in a time not exceeding the next frame duration. For example, to maintain a 10 Hz frame rate, the computer must capture and compute 14,400 1k-point FFTs within 100 ms. The corresponding total raw sample rate is thus 147.4 M samples per second. Acquiring and processing such a high data rate in real time is very demanding. This is achieved using a parallelized multi-threaded C code running on a mid-level desktop PC (i7-4770S quad-core 8 thread processor, clocked at 3.1 GHz with 32 GB RAM). Samples are transferred from the ADC threads to the FFT threads directly as integer values. Conversion to floating point, nonlinearity compensation, windowing, FFT, power conversion and data reordering of the scan pattern are all performed within the FFT threads.

Imagery is displayed in real time as 2D images of the maximum intensity per line of sight for simplicity. Rendering is performed on the PC's GPU using the OpenGL graphics interface. Power spectrum data is uploaded to the GPU as 32-bit float *textures*, with coordinate translation, conversion to decibels and color-scaling performed using OpenGL *shaders*.

Data can also be saved to disk for offline analysis, either as raw time series data or as truncated range spectra from the sense volume. Due to the sheer quantity of raw time series integer data (29 MB per frame), saving in real time (i.e. at the

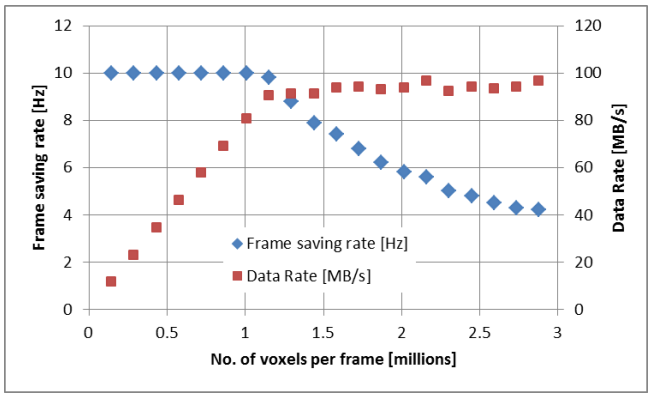

Fig. 9. Frame saving rate and data rate as a function of number of millions of voxels per frame.

same rate as images are being acquired) is only possible at frame rates of less than 1 Hz. For range spectra, the full output data cube of 144 x 100 x 200 = 2.88 million voxels amounts to 23 MB per frame of 64-bit floating point values. Being floating point values, range spectra occupy more memory per point than the raw input integer values but voxels which contain no information outside of the target volume can be discarded. The data saving rate therefore depends on the degree to which the output data cube is truncated. For testing purposes, one can reduce the range spectra data set by limiting the number of range bins which are saved. Fig. 9 shows how the frame saving rate rises as the number of voxels per frame is reduced from the nominal 2.88 million. For example, one can maintain 10 Hz real time operation if only 1 million voxels per frame are saved i.e. 70 range bins, a range swath of just 35 cm. Fig. 9 also shows how the data rate during saving plateaus at about 93 MB/s for frames containing >1 million voxels. However, in practice, we do not wish to truncate the range extent so an adaptive thresholding algorithm will be used to truncate the data by amplitude. It is anticipated that this method will be able to reduce the amount of data transmitted (over Ethernet) to the AAD PC to 10% of the full data cube and thus maintain real time operation at 10 Hz frame rate.

IV. Example Imagery

The radar subsystem has been installed in the CONSORTIS system enclosure – Fig. 10. The space underneath the radar is for the dual-band passive imager.

Currently, the radar operates at a frame rate of 7 Hz rather than 10 Hz to avoid a timing synchronization problem at the start of each acquisition which occurs at higher speeds caused by USB timing latency. For testing, imagery can be collected and displayed for the whole target volume in bursts of up to ~250 frames, limited by the available RAM. At 7 Hz this represents a burst duration of over 30 seconds. Offline analysis and post-processing is conducted in MATLAB. For the envisaged airport security deployment, images will be acquired in much shorter bursts and conveyed to the AAD for analysis with low latency.

As noted in section II D, the scan pattern is non-uniform and this is illustrated in Fig. 11 (Left) which displays each actual sampling direction as a dot color coded by maximum

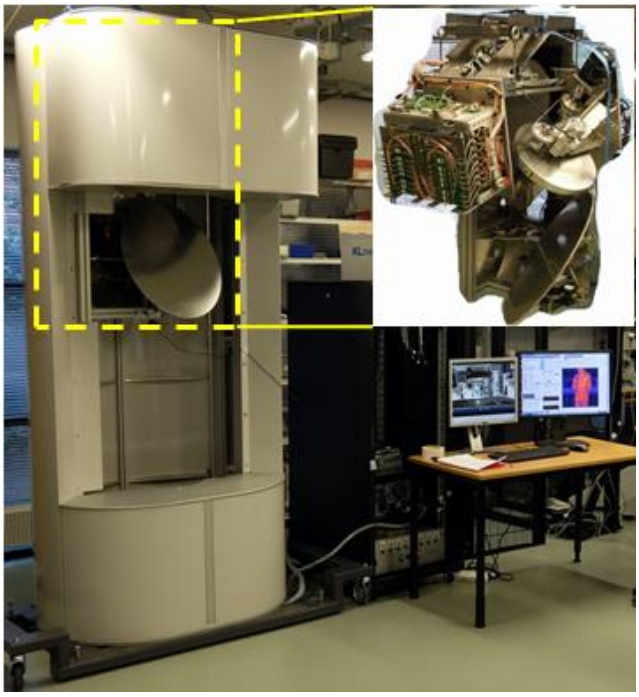

Fig. 10. The CONSORTIS system enclosure showing the location of the radar subsystem and the radar itself (inset).

return power along each line of sight. The subject is a man holding a 12 x 12 cm slab of absorbing plastic. The figure-of-eight scan pattern, which in this case is for an up frame, is clearly evident. Some transceivers have a higher noise floor than others so in lines of sight not occupied by the person these noise floors appear as dark blue bands. The color scale represents a dynamic range of 60 dB.

When the actual angular sampling positions are interpolated onto a 144 x 100 rectangular grid the resulting maximum intensity image is shown in Fig. 11 (Center). The high spatial resolution of order 1 cm resolves subject features well. Specular reflections are evident from skin and clothing when the local surface is normal to the incident beam. In this image only 70 range bins were saved so the man's face and hand were truncated and hence appear as low intensity.

An alternative presentation for the data is to color code by range bin which is shown in Fig. 11 (Right) in which pale colors represent closer ranges. The color scale represents 70 range bins or 35 cm. The data have been thresholded to exclude the background based on a histogram analysis of the reflected power values. With the nonlinearity compensation described above the full range resolution offered by the 30 GHz chirp bandwidth is realized.

The analysis and interpretation of this type of 3D radar data is the subject of ongoing work. Other 2D visualizations such as point clouds and surface reconstructions are possible. It is worth noting that whilst these are single frame images, the radar outputs 3D movies with multi-hertz frame rates and this offers the possibility of frame-to-frame analysis for enhanced anomaly detection. The radar is being integrated with the rest of the CONSORTIS system and will then undergo data collection trials.

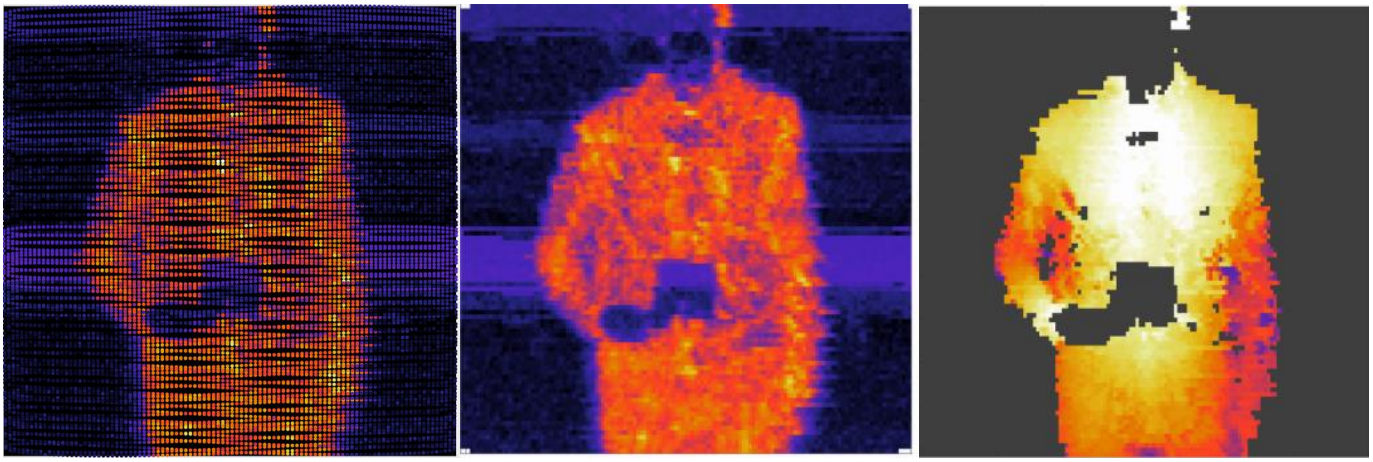

Fig. 11. Dot plot of actual sampling directions with color coding by maximum return power along each line of sight (Left). Single frame image interpolated onto rectangular grid accounting for actual scan pattern, color coded by maximum intensity over a 60 dB range (Center) and color coded by range bin number over 70 range bins / 35 cm (Right).

The ultimate goal is for the AAD processor, which runs on a separate PC, to make automatic detections from the radar data, which will ensure reliable detection and the privacy of the subject, but that work is ongoing.

V. CONCLUSIONS

A 340 GHz 16-channel FMCW radar has been developed for next-generation airport security applications. The radar maps the subject in 3D with ~1cm^3 voxel resolution over a 1m^3 sense volume at multi-hertz frame rates. This performance is achieved by combining advanced transceiver electronics with high speed mechanical beam steering and parallelized processing. When the radar is combined with the dual-band passive submillimeter wave imager and automatic anomaly detection software, the CONSORTIS system aims to demonstrate high resolution, real time security imaging with significantly improved throughput rates whilst respecting the privacy of the public.

ACKNOWLEDGMENT

Part of the research leading to these results has received funding from the European Union Seventh Framework Programme (FP7/2007-2013) under grant agreement no. 312745. The authors are very grateful to all our colleagues in the CONSORTIS project for their ongoing support and collaboration.

REFERENCES

[1] Schouten, P., "Security as controversy: Reassembling security at Amsterdam Airport", Security Dialogue, vol. 45, February 2014, pp. 23 – 42.

[2] http://www.sds.l-3com.com/products/advancedimagingtech.htm

[3] https://www.smithsdetection.com/products/eqo/

[4] https://www.rohde-schwarz.com/uk/product/qps-productstartpage_63493-332676.html

[5] CONSORTIS website: http://consortis.eu/.

[6] Cooper, K.B., et al., "THz Imaging Radar for Standoff Personnel Screening," IEEE Trans. Terahertz Science and Technology, vol. 1, no. 1,2011, pp. 169 – 182.

[7] Robertson, D.A., Marsh, P.N., Bolton, D.R., Middleton, R.J.C., Hunter, R.I., Speirs, P.J., Macfarlane, D.G., Cassidy, S.L., and Smith, G.M., "340 GHz 3D radar imaging test bed with 10 Hz frame rate.", Proc. SPIE 8362, Passive and Active Millimeter-Wave Imaging XV, 2012, 836206.

[8] Grajal, J., Badolato, A., Rubio-Cidre, G., Ubeda-Medina, L.; Mencia-Oliva, B., Garcia-Pino, A., Gonzalez-Valdes, B., and Rubinos, O, "3-D High-Resolution Imaging Radar at 300 GHz With Enhanced FoV", IEEE Trans. Microwave Theory Tech., vol. 63, no. 3, 2015, pp. 1097-1107.

[9] Robertson, D. A., Macfarlane, D. G. & Bryllert, T., "220GHz wideband 3D imaging radar for concealed object detection technology development and phenomenology studies", Proc. SPIE 9830, Passive and Active Millimeter-Wave Imaging XIX., Apr. 2016, pp. 1-8.

[10] Robertson, D.A. et al, "High resolution, wide field of view, real time 340GHz 3D imaging radar for security screening", Proc. SPIE 10189, Passive and Active Millimeter-Wave Imaging XX., Apr. 2017, 101890C.

[11] Dahlbäck, R., Bryllert, T., Granström, G., Ferndahl, M. Drakinskiy, V. and Stake, J., "Compact 340 GHz homodyne transceiver modules for FMWC imaging radar arrays," IEEE MTT-S International Microwave Symposium (IMS), 2016, pp. 1 – 4.